# Highly Efficient Tandem Polymer Photovoltaic Cells

**ARTICLE** *in* ADVANCED MATERIALS · JANUARY 2010

Impact Factor: 17.49 · DOI: 10.1002/adma.200901624 · Source: PubMed



**8 AUTHORS**, INCLUDING:

Ziruo Hong
University of California, Los Angeles
**129** PUBLICATIONS **7,516** CITATIONS
SEE PROFILE

Yue Wu
Solarmer Energy Inc.
**21** PUBLICATIONS **7,122** CITATIONS
SEE PROFILE

Gang Li
University of California, Los Angeles
**143** PUBLICATIONS **22,930** CITATIONS
SEE PROFILE

COMMUNICATION

# Highly Efficient Tandem Polymer Photovoltaic Cells

By *Srinivas Sista, Mi-Hyae Park, Ziruo Hong,* Yue Wu, Jianhui Hou, Wei Lek Kwan, Gang Li,* and *Yang Yang**

Polymer tandem cells have spurred much interest because of their advantage to harvest a greater part of the solar spectrum. However, the working mechanism of the interlayer that joins the two subcells in a tandem cell is less understood and is essential in achieving high efficiency. In this manuscript, we study the role of the n-type and p-type layers constituting the interlayer and several important issues of the tandem structure, including optical optimization, interfacial engineering, and accurate efficiency characterization. Closer inspection of the interlayer, which consists of a n-type nanocrystalline $TiO_2$ layer and a p-type conducting polymer layer, reveals that it acts as a metal/semiconductor contact as opposed to a tunnel junction in inorganic tandem cells. Here, we demonstrate that high-efficiency tandem cells with power conversion efficiencies (PCE) of 5.84% can be achieved by using the efficient interlayer characteristics. Furthermore, a highly conductive interlayer should be avoided for accurate device efficiency characterization, which otherwise leads to overestimation of efficiencies. The understanding developed in this Communication can be expected to further enhance the efficiency of tandem cells with large bandgap polymers.

Organic solar cells have attracted much attention in the past decade, mainly because of their application potential in a next generation of renewable energy resources.[1–3] Significant improvement in polymer photovoltaic cells has been achieved recently with the synthesis of new donor polymers that can reach a PCE higher than 5% when blended with the methanofullerene [6,6]-phenyl–$C_{61}$–butyric acid methyl ester (PCBM).[4–10] However, the narrow absorption range of the donor polymers leaves a major part of solar spectrum non-utilized. To achieve a broad absorption, tandem structures have been employed by stacking of two or more bulk heterojunctions (BHJs)[11] with complementary absorption spectra. For a series connection of two cells, the open circuit voltage ($V_{oc}$) of the tandem cell is the sum of $V_{oc}$ of the two subcells, while the overall current is limited by the subcell with the smaller current. With this strategy, tremendous efforts have been devoted to the development of desirable device configurations and interlayers through various methods[12–14] and tandem cells with a PCE over 6% have been achieved.[15] However, since then there has been little progress in polymer tandem cells, mainly due to the complicated processing and the lack of understanding of the working mechanism in such a dual-BHJ system.

Several criteria need to be considered in order to achieve highly efficient tandem devices; these include minimal absorption overlap between the two subcells, a compatible fabrication process for constructing a layer-by-layer structure, and an efficient interlayer for connecting the subcells. Our work delves into the understanding of the physics of an efficient interlayer and the role of n-type $TiO_2$ and p-type poly(3,4-ethylenedioxythiophene) poly(styrenesulfonate) (PEDOT:PSS) materials. $TiO_2$ synthesized via a non-hydrolytic sol–gel process offers a simple way to control the nanocrystal size and fabricate a film by eliminating thermal-annealing and hydrolysis treatment in air.[16] On the $TiO_2$ surface the PEDOT:PSS film (conductivity of $10^{-3}$ S cm$^{-1}$) acts as an anode for the rear cell. Utilization of PEDOT4083, instead of highly conductive PEDOT:PSS (PH500), allows accurate evaluation of the active area of photovoltaic cells and thus overall efficiencies, as discussed later in detail.

In our tandem structure, poly(3-hexylthiophene) (P3HT) with a bandgap of 1.9 eV is used as a front cell. One advantage of P3HT:$PC_{70}$BM BHJs is that its short-circuit current density ($J_{sc}$) can be easily and precisely tuned by changing its thickness, while $V_{oc}$ and fill factor (FF) remain constant, thereby allowing photocurrent balance between the subcells. The rear cell consists of a lower band gap (1.5 eV) polymer, poly[(4,4′-bis(2- ethylhexyl) dithieno[3,2-*b*:2′,3′-d]silole)-2,6-diyl-*alt*-(2,1,3-benzothiadiazole)-4,7-diyl] (PSBTBT).[8] The PCE of a PSBTBT:$PC_{70}$BM single cell increases by 10% when the incident light is reduced from 1 sun to $^1/_2$ sun because of reduced non-geminate recombination (see Supporting Information, SI-[A], Fig. SI-1). This property of PSBTBT allows for the use as a rear subcell since the light intensity received by the rear subcell is attenuated by ~40% after passing through the front P3HT:PCBM subcell.

The device configuration and the proposed energy level diagram of the tandem photovoltaic cell are shown in Figure 1a and b, respectively. The absorbance of the tandem cell without a cathode reaches an optical density of over 0.8 in the spectral range 350–600 nm, where the absorption of the two BHJs overlaps, whereas the absorbance value reaches 0.3 at 750 nm corresponding to rear cell absorption, as shown in Figure 1c. This suggests that over 50% of incident light from 650 to 790 nm is absorbed in the presence of a reflective cathode. Optical simulation was performed to calculate the absorption profile for matching the absorption of the two subcells (see Supporting Information Fig. SI-2 for refraction indices ($n$) and extinction coefficients ($k$) derived from ellipsometry measurements).[17] According to the

[*] Dr. Z. Hong, Prof. Y. Yang, S. Sista, M.-H. Park, Dr. Y. Wu, Dr. J. Hou, W. L. Kwan
Department of Materials Science and Engineering
University of California Los Angeles
Los Angeles, CA 90095 (USA)
E-mail: zrhong@ucla.edu; yangy@ucla.edu
Dr. Y. Wu, Dr. J. Hou, Dr. G. Li
Solarmer Energy, Inc.
El Monte, CA 91731 (USA)

DOI: 10.1002/adma.200901624

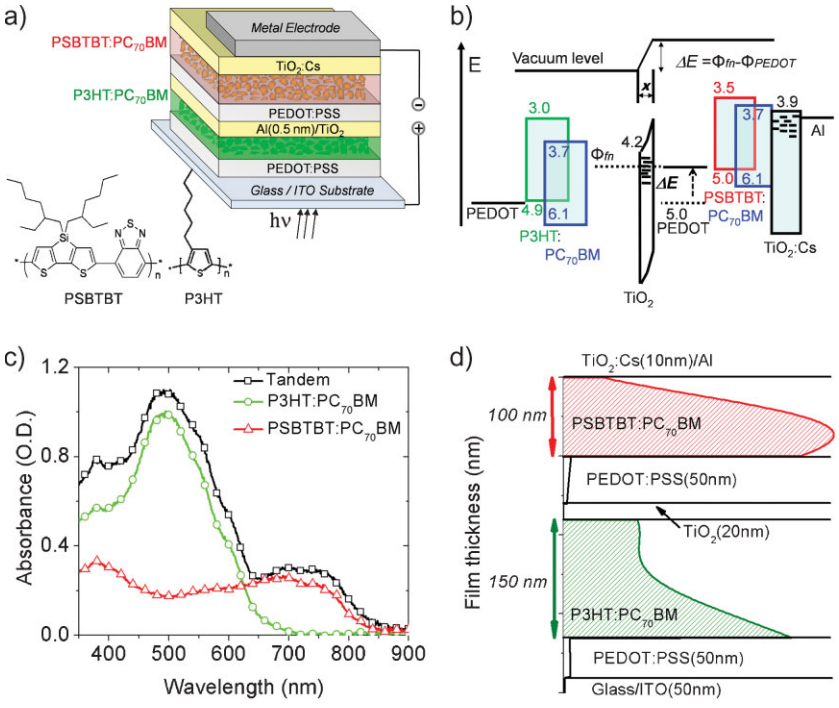


**Figure 1.** a) Device configuration and b) proposed energy level diagram of tandem solar cells containing two BHJs as subcells and $TiO_2$/PEDOT4083 as an interconnection layer. c) absorbance (optical density, O.D.) of P3HT:$PC_{70}BM$ and PSBTBT:$PC_{70}BM$ BHJ films and tandem photovoltaic cells without reflective cathode. d) Calculated absorption profile of the tandem cell under AM1.5G illumination.

optical simulation results shown in Figure 1d, a 100-nm PSBTBT:$PC_{70}BM$ film absorbs 15% more photon flux than the front P3HT:$PC_{70}BM$ cell under illumination of AM1.5G. Therefore, the P3HT front cell limits the overall photocurrent, and hence the FF of tandem cells. A 10-nm layer of $TiO_2$:Cs was inserted between the Al cathode and PSBTBT:$PC_{70}BM$ BHJ for efficient electron extraction.[16]

The current density versus voltage ($J$–$V$) characteristics of the tandem and reference single cells were taken under AM1.5G 100 mW $cm^{-2}$ illumination as shown in Figure 2a and photovoltaic parameters are listed in Table 1. The tandem cell yields a PCE of 5.84% with a $V_{oc}$ of 1.25 V. From P3HT:$PC_{70}BM$ BHJs with a thickness of 150 nm PCE of 3.77% is obtained with a $J_{sc}$ of 9.27 mA $cm^{-2}$. The low-bandgap PSBTBT:$PC_{70}BM$ BHJ with a thickness of 100 nm exhibits a $J_{sc}$ of 10.71 mA $cm^{-2}$ and a PCE of 3.94%.

The external quantum efficiency (EQE) of the tandem cell and single cells as reference was measured using the method proposed by Kim et al.,[15] as shown in Figure 2b. However, it should be noted that EQE measurements using this method are appropriate only for cases in which the two subcells exhibit large enough shunt resistance (see Supporting Information, SI-[C]). The EQE curve of the reference cell based on P3HT:PCBM has an average value of over 50% throughout the visible range, due to strong absorption of both P3HT and $PC_{70}BM$. The photoresponse of the single PSBTBT:$PC_{70}BM$ cell is consistent with our previous report,[8] showing a broad response range from 350 to 800 nm with a maximum of over 40% at 700 nm. Integration of the EQE curves under the AM1.5G solar spectrum yields $J_{sc}$ values consistent with the $J$–$V$ curves shown in Figure 2a.

We modified the surface of the P3HT:$PC_{70}BM$ film by depositing an ultrathin Al (UT-Al) layer, improving both the wettability and electrical contact of the $TiO_2$ film on the P3HT:$PC_{70}BM$ film. The resulting $TiO_2$ film consists of a densely packed network of $TiO_2$ nanocrystals (see SI-[D], Fig. SI-3), which is able to prevent penetration of subsequently deposited layers, therefore, collecting electrons and blocking holes with a high selectivity. This is critical to preserve $V_{oc}$ of tandem cells.

As listed in Table 1, $V_{oc}$ of the tandem cell approaches the sum of the two reference cells, suggesting effectiveness of the interlayer. From the dark $J$–$V$ curves of a fresh tandem cell shown in Figure 3a, we noted that the rectification ratio at ±2.0 V is only ~10, although the tandem cells with such poor diode behavior show a PCE of 5.84%. This rectification ratio improved by two orders of magnitude after illumination. The reason is tentatively attributed to the photoconductivity of $TiO_2$. To confirm this, the $J$–$V$ characteristics under illumination with and without a 400-nm cutoff filter, which completely blocks the UV part of the solar spectrum, were measured and are shown in Figure 3b. When the device is illuminated without any UV photons, a significant hump, so-called "S-shape", near $V_{oc}$ was observed.[18] This S-shape should be related to an interfacial barrier for charge transport.[19] Interestingly, when the cutoff filter is removed, the S-shape disappears and is not observed even when the cutoff filter is added again. This phenomenon is observed only when UV-light is cut off, implying that $TiO_2$ is the origin, while this observation cannot be considered merely as photoconductivity.[20]

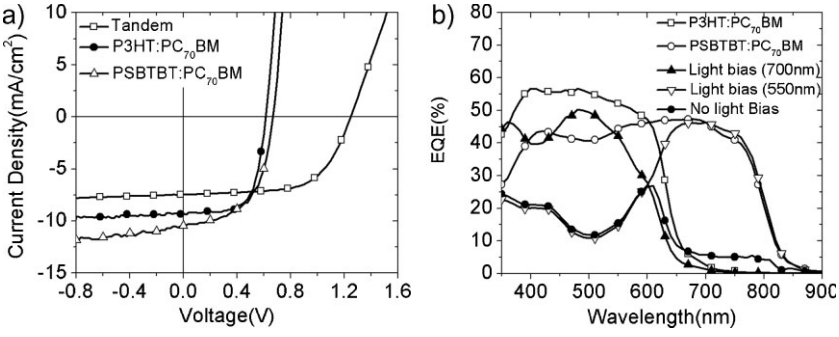


**Figure 2.** a) $J$–$V$ characteristics of a tandem and reference single cells measured under standard AM1.5G 100 mW $cm^{-2}$ illumination. b) EQE of subcells in a tandem structure (with and without monocolor light bias) and reference single cells.

**Table 1.** Photovoltaic performance of reference single cells and a tandem cell.

| Device | PCE | $V_{oc}$ | $J_{sc}$ | FF |
|---|---|---|---|---|
| | [%] | [V] | [mA cm$^{-2}$] | [%] |
| **P3HT:PC$_{70}$BM** | 3.77 | 0.60 | 9.27 | 66.6 |
| **PSBTBT:PC$_{70}$BM** | 3.94 | 0.67 | 10.71 | 55.8 |
| **Tandem** | 5.84 | 1.25 | 7.44 | 63.2 |

A similar phenomenon is observed for a P3HT:PC$_{70}$BM single cell with UT-Al/TiO$_2$/PEDOT4083/Al as the cathode, as shown in Figure 3a and b. It can be seen that inserting PEDOT4083 between the TiO$_2$ layer and the Al cathode has a negligible influence on the *J–V* characteristics. Considering Ohmic contact between Al and PEDOT4083, a UV-induced Schottky-to-Ohmic transition of the PEDOT4083/TiO$_2$ contact appears. TiO$_2$ has an electron quasi-Fermi level near to the LUMO level of PCBM and, on the other hand, PEDOT4083 is a heavily p-doped conductive polymer, which can be regarded as a high work-function metal. Therefore, TiO$_2$/PEDOT4083 can be considered as a metal/semiconductor contact that forms a triangular barrier as shown in Figure 1b. In case of a large width of the triangular barrier due to a small carrier concentration in TiO$_2$ upon Fermi-level alignment, both extraction and injection of electrons are blocked, resulting in the S-shape in absence of UV light. Upon shining UV light, the free carrier concentration in TiO$_2$ significantly increases, leading to narrowing of the triangular barrier width that is thin enough for efficient tunneling of electrons through the triangular barrier. This is equivalent to having no energy barrier across the TiO$_2$/PEDOT4083 interface, which explains the observed increase in the forward bias current by two orders of magnitude upon exposure to UV light. Unfortunately, the carrier density and the conductivity of TiO$_2$ nanocrystals is difficult to characterize quantitatively at the moment and further efforts on quantifying charge carrier dynamics and determining the recombination zone in the interlayer are under way.

The nature of the interlayer for our polymer tandem cells, which has not been clearly investigated so far, is established to behave as a metal/semiconductor junction, i.e., a Schottky contact. The contact properties of TiO$_2$/PEDOT4083 are believed to be determined by photogenerated electrons in the TiO$_2$ layer induced by UV light. Unlike the highly doped p–n junction for carrier tunneling without any potential loss in inorganic tandem cells,[21] the TiO$_2$/PEDOT4083 interface in the single cell of ITO/PEDOT4083/P3HT:PC$_{70}$BM/UT-Al/TiO$_2$/PEDOT4083/Al showed a normal diode behavior with a significant rectification, as shown from the dark *J–V* curve in Figure 3a, because the n-type TiO$_2$ layer transports electrons only and a hole injection into TiO$_2$ is energetically forbidden.

Another important concern that needs to be addressed is the effect of conductivity of the PEDOT:PSS layer on the active area of the device. Figure 3c shows the *J–V* characteristics under light illumination of the devices, ITO/PEDOT4083/P3HT:PC$_{70}$BM/UT-Al/TiO$_2$/ PEDOT:PSS/Al. When PH500 is used for a second PEDOT:PSS layer, $J_{sc}$ increases to 11.2 mA cm$^{-2}$, which is nearly 20% higher than the $J_{sc}$ of the control device with PEDOT4083, while no difference of EQE for the two cells was observed. The increased $J_{sc}$ is ascribed to the high conductivity of PH500 films, 5–10 S cm$^{-1}$, which causes a larger active area than the electrode overlap. We defined the active area by scratching the PH500 layer along the edge of the Al cathode and the $J_{sc}$ was reduced to 9.5 mA cm$^{-2}$. The tandem cell using PH500 as an interlayer reaches a PCE of 6.01%; however, after re-defining the effective area, the efficiency also drops to 5.44%, as shown in Figure 3d. A $J_{sc}$ of the tandem cell of over 9 mA cm$^{-2}$, which is ~20% higher than $J_{sc}$ obtained by EQE, supports that the PH500 layer increases the active area of the front cell.[22] In this case, the rear subcell becomes the photocurrent-limiting cell, giving a low FF of 55% for tandem cells.[23] After scratching, the front cell limits the overall photocurrent, resulting in a FF higher than 60%. According to our observation, extra care over efficiency estimation has to be taken when using highly conductive materials in the interlayer.

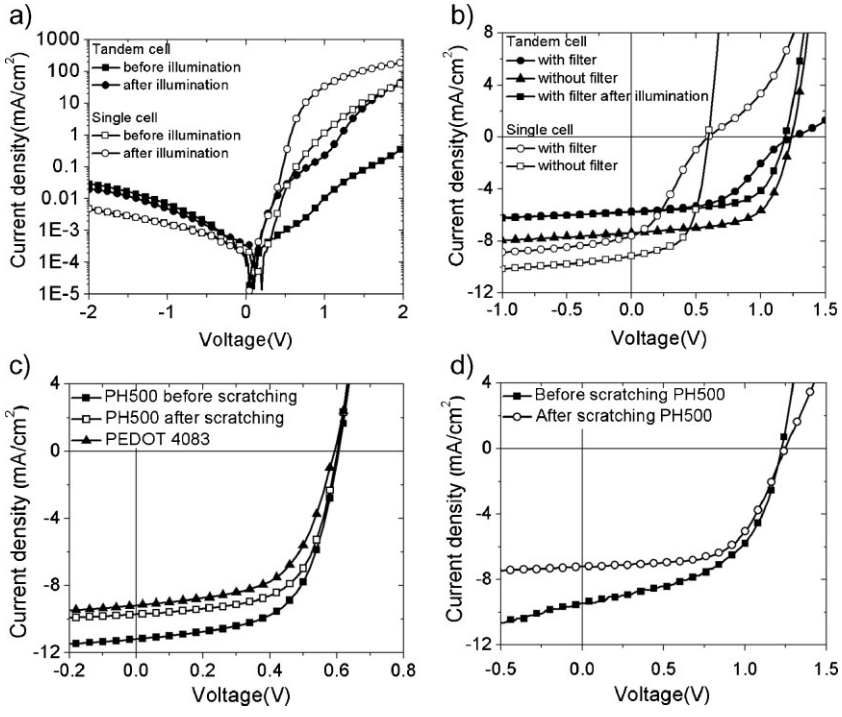


**Figure 3.** a) Dark *J–V* characteristics of a tandem cell and a single cell (ITO/PEDOT/P3HT:PC$_{70}$BM/UT-Al/TiO$_2$/PEDOT4083/Al) before and after illumination. b) *J–V* characteristics of tandem cells and single cells under illumination with and without a 400-nm cutoff filter. c) *J–V* characteristics under illumination of single cells with the structure ITO/PEDOT4083/P3HT:PC$_{70}$BM/UT-Al/TiO$_2$/PEDOT:PSS/Al using either PEDOT4083 or highly conductive PH500. d) A tandem cell using PH500 as an interlayer before and after defining an active area by scratching.

In summary, we demonstrate an efficient photovoltaic cell with a tandem structure. Mechanism studies indicate that a metal/

semiconductor contact between the conductive polymer and the semiconducting metal oxide, which connects individual subcells in a series, works effectively as an interlayer. It is worth emphasizing that the front cell with a larger bandgap should offer higher $V_{oc}$ to explore the full potential of the tandem cells.[24] In this sense, P3HT is used mainly to demonstrate the concept, rather than efficiency improvement, because large bandgap of P3HT offers a mediocre $V_{oc}$ of 0.6 V. With a suitable combination of donor–acceptor systems, which are able to deliver higher $V_{oc}$ from the front cell[25] and all other parameters remaining the same as for P3HT, the PCE of tandem cells can be significantly improved.

## Experimental

*Device Fabrication*: Photovoltaic cells were fabricated on indium tin oxide (ITO) coated glass substrates with a sheet resistance of 15 Ω square$^{-1}$. The PEDOT:PSS (VP AI 4083 from H. C. Stark, PEDOT4083) layer was spin-casted at 4000 rpm for 60 s and annealed at 140 °C for 15 min. The P3HT:$PC_{70}BM$ at a 1:0.7 weight ratio in 1% chloroform solution was spin-casted at 4000 rpm for 30 s on top of a layer of PEDOT 4083. The films were annealed at 150 °C for 30 min. After thermal evaporation of 5 Å Al in vacuum, a thin layer of n-type nanocrystalline $TiO_2$ film was spin-casted from 0.25 wt% of $TiO_2$ solution in a 1:1 volume ratio of 2-ethoxyethanol and ethanol at 1000 rpm, followed by thermal annealing at 120 °C for 10 min. After spin-coating of a second PEDOT:PSS layer, PSBTBT:$PC_{70}BM$ (1:1.5) from 1% chloroform solution was drop-cased, while the substrate was spinning at 4500 rpm and another thermal annealing step was performed at 140 °C for 5 min. Finally, a $TiO_2$:Cs solution prepared by blending 0.5 and 0.2 wt% solutions of $TiO_2$ and $Cs_2CO_3$ in a 1:1 volume ratio was spin-casted at 3000 rpm for 30 s, and the thermal annealing was performed at 80 °C for 20 min. The device fabrication was completed by thermal evaporation of 80 nm Al as the cathode under vacuum at a base pressure of $2 \times 10^{-6}$ Torr.

*Electrical, Optical and Microscopic Characterization of Photovoltaic Cells and Thin Films*: Absorption spectra were taken using a Varian Cary 50 ultraviolet–visible spectrophotometer. The *n* and *k* values for the different layers in the tandem cell were measured using an ellipsometer and the values obtained were fed into the software to get the optical field profile. *J–V* characteristics of photovoltaic cells were taken using a Keithley 4200 source unit under a simulated AM1.5G spectrum with an Oriel 9600 solar simulator. Atomic force microscopy (AFM) images were taken on a digital instruments multimode scanning probe microscope. For EQE and X-ray/UV photoelectron spectroscopy (XPS/UPS) measurements refer to SI-[C] and [D], respectively.

## Acknowledgements

S.S. and M.-H.P. contributed equally to this work. Authors are grateful to H.-Y. Chen of University of California Los Angeles (UCLA) for device processing of the low bandgap polymer (PSBTBT), Dr. L. J. Huo of UCLA for supplying PSBTBT, L.-M. Chen and Dr. Z. Xu of UCLA for UPS measurement, W. Lin from UCLA Nanoelectronics Research Facility and L. Kitzinger from SOPRA Inc. for Ellipsometry experiment. This work was financially supported by the Air Force Office of Scientific Research (Grant No. FA9550-07-1-0264), Office of Naval Research (Grant No. N00014-04-1-0434), and Solarmer Energy Inc. (Grant No. 20061880). Supporting Information is available online from Wiley InterScience or from the author.

Received: May 15, 2009
Revised: June 20, 2009
Published online: September 23, 2009

[1] C. W. Tang, *Appl. Phys. Lett.* **1986**, *48*, 183.
[2] H. Hiramoto, H. Fujiwara, M. Yokoyama, *Appl. Phys. Lett.* **1991**, *58*, 1062.
[3] N. S. Sariciftci, D. Braun, C. Zhang, V. I. Srdanov, A. J. Heeger, G. Stucky, F. Wudl, *Appl. Phys. Lett.* **1993**, *62*, 585.
[4] F. Padinger, R. S. Rittberger, N. S. Sariciftci, *Adv. Funct. Mater.* **2003**, *13*, 85.
[5] G. Li, V. Shrotriya, J. Huang, Y. Yao, T. Moriarty, K. Emery, Y. Yang, *Nat. Mater.* **2005**, *4*, 864.
[6] M. S. White, D. C. Olson, S. E. Shaheen, N. Kopidakis, D. S. Ginley, *Appl. Phys. Lett.* **2006**, *89*, 143517.
[7] J. Peet, J. Y. Kim, N. E. Coates, W. L. Ma, D. Moses, A. J. Heeger, G. C. Bazan, *Nat. Mater.* **2007**, *6*, 497.
[8] J. H. Hou, H.-Y. Chen, S. Zhang, G. Li, Y. Yang, *J. Am. Chem. Soc.* **2008**, *130*, 16144.
[9] Y. Liang, Y. Wu, D. Feng, S.-T. Tsai, H.-J. Son, G. Li, L. Yu, *J. Am. Chem. Soc.* **2009**, *131*, 56.
[10] S. H. Park, A. Roy, S. Beaupré, S. Cho, N. Coates, J. S. Moon, D. Moses, M. Leclerc, K. Lee, A. J. Heeger, *Nat. Photonics* **2009**, *3*, 297.
[11] A. Hadipour, B. de Boer, P. W. M. Blom, *J. Appl. Phys.* **2007**, *102*, 074506.
[12] J. Drechsel, B. Mannig, F. Kozlowski, M. Pfeiffer, M. Leo, H. Hoppe, *Appl. Phys. Lett.* **2005**, *86*, 244102.
[13] J. Gilot, M. M. Wienk, R. A. J. Janssen, *Appl. Phys. Lett.* **2007**, *90*, 143512.
[14] M. Hiramoto, M. Suezaki, M. Yokoyama, *Chem. Lett.* **1990**, *19*, 327.
[15] J. Y. Kim, K. Lee, N. E. Coates, D. Moses, T.-Q. Nguyen, M. Dante, A. J. Heeger, *Science* **2007**, *317*, 222.
[16] M.-H. Park, J.-H. Li, A. Kumar, G. Li, Y. Yang, *Adv. Funct. Mater.* **2009**, *19*, 1241.
[17] D. W. Sievers, V. Shrotriya, Y. Yang, *J. Appl. Phys.* **2006**, *100*, 114509.
[18] A. Kumar, S. Sista, Y. Yang, *J. Appl. Phys.* **2009**, *105*, 094512.
[19] C. Uhrich, R. Schueppel, A. Petrich, M. Pfeiffer, K. Leo, E. Brier, P. Kilickiran, P. Baeuerle, *Adv. Funct. Mater.* **2007**, *17*, 2991.
[20] N. Golego, S. A. Studenikin, M. Cocivera, *Phys. Rev. B* **2000**, *61*, 8262.
[21] J. M. Olson, S. R. Kurtz, A. E. Kibbler, P. Faine, *Appl. Phys. Lett.* **1990**, *56*, 623.
[22] A. Cravino, P. Schilinsky, C. J. Brabec, *Adv. Funct. Mater.* **2007**, *17*, 3906.
[23] A. Hadipour, B. de Boer, P. W. M. Blom, *Org. Electron.* **2008**, *9*, 617.
[24] G. Dennler, M. C. Scharber, T. Ameri, P. Denk, K. Forberich, C. Waldauf, C. J. Brabec, *Adv. Mater.* **2008**, *20*, 579.
[25] R. B. Ross, C. M. Cardona, D. M. Guldi, S. G. Sankaranarayanan, M. O. Reese, N. Kopidakis, J. Peet, B. Walker, G. C. Bazan, E. Van Keuren, B. C. Holloway, M. Drees, *Nat. Mater.* **2009**, *8*, 208.